Localization of Stimulated Brillouin Scattering in Random Phase Plate Speckles

H. A. Baldis,[2] C. Labaune,[1] J. D. Moody,[3] T. Jalinaud,[1,*] and V. T. Tikhonchuk[4,†]

[1]*Laboratoire pour l'Utilisation des Lasers Intenses, Ecole Polytechnique, Centre National de la Recherche Scientifique, 91128 Palaiseau cedex, France*

[2]*Institute for Laser Science and Applications (ILSA), Lawrence Livermore National Laboratory, P.O. Box 808, Livermore, California 94550*

[3]*Lawrence Livermore National Laboratory, P.O. Box 808, Livermore, California 94550*

[4]*Centre de Physique Théorique, Ecole Polytechnique, Centre National de la Recherche Scientifique, 91128 Palaiseau cedex, France*

(Received 22 September 1997)

This paper presents the first experimental evidence of the transverse localization of stimulated Brillouin scattering (SBS) emission to the laser beam axis, demonstrating that only a few small regions of plasma contribute to the emission. As a consequence, SBS reflectivity of these regions is much higher than the average SBS reflectivity, by a factor of $\sim 50-100$. These observations are consistent with the recent concept of SBS growing mainly in "active" speckles, having an intensity higher than the average laser intensity. [S0031-9007(98)05456-8]

PACS numbers: 52.35.Nx, 52.35.Fp, 52.40.Nk, 52.50.Jm

Stimulated Brillouin scattering (SBS) is a parametric instability which can occur during the propagation of an intense laser beam through a plasma in the presence of ion density fluctuations [1,2]. This instability is of crucial importance in inertial confinement fusion (ICF) because it can induce significant losses of the incident laser energy and spoil the illumination symmetry required to reach good implosion efficiency of the pellet. Stimulated Brillouin scattering is the resonant decay of the incident electromagnetic wave (EMW) into a scattered EMW and an ion acoustic wave (IAW). Characterization of the total, or macroscopic, SBS reflectivity is important to ICF, but in spite of the efforts during the last twenty years, it has been very difficult to match measured and calculated SBS reflectivities averaged over space and time. More detailed characterization of local SBS reflectivity is extremely important if one is to extrapolate with confidence the role of scattering instabilities to the large plasmas encountered in the national ignition facility targets [3], and to develop methods for controlling them.

We present in this paper the first experimental evidence of the localization of SBS emission, in a plane perpendicular to the laser beam axis, demonstrating that only a few small interaction regions contribute to the total SBS light. SBS emission from these small spots has been evaluated leading to local reflectivities much higher than the average SBS reflectivity, by a factor of ~ 100. These observations are consistent with the recent concept of convective amplification of SBS in randomly distributed speckles [4] as produced by a random phase plate (RPP) [5]. This new approach is important as it can explain the moderate observed average SBS reflectivities because of the limited number of SBS-active speckles, and pump depletion within these speckles. Application of the statistical theory has been successful in explaining a number of different physical features of SBS in a recent experiment [6]. The observation of localized regions of SBS emission presented in this paper demonstrates the importance of the microscopic description of SBS.

The use of a RPP on the beam which pumps the SBS instability is an important component of the present study, not only because it provides beam smoothing and reproducible experimental conditions, but also because it produces a small-scale intensity distribution in the focal volume which can be described by a statistical function. A RPP is a transparent substrate with a random pattern of phase elements that introduce a phase shift of 0 or π on the incident light. The far-field intensity distribution consists of an overall envelope determined by an individual phase plate element. Within this envelope, there is a fine-scale speckle structure due to the interferences between different phase element contributions, whose dimensions are determined by the f/number of the focusing optics. The advantage of this technique is that it creates a well-defined intensity distribution in the laser focal spot which is nearly independent of aberrations of the initial laser beam. Within the focal region, however, there are large amplitude laser intensity fluctuations in a speckle scale length, randomly distributed, which manifest themselves in fluctuations on the SBS growth and reflectivities as discussed in this paper. The overall SBS reflectivity is the sum of contributions from the individual speckles.

The experiments have been performed using two beams of the laser facility of the Laboratoire pour l'Utilisation des Lasers Intenses (LULI) at Ecole Polytechnique. One beam, with wavelength 1.053 μm, was used to preform a plasma by irradiating CH foils 500 nm thick, using an $f/8$ focusing lens. The second beam, with wavelength $\lambda_0 = 0.53$ μm, was the interaction beam, with a delay of 300 ps, and an angle of 45°, with respect to the plasma forming beam. Both laser pulses have a full width at half maximum (FWHM) duration of 600 ps. The interaction beam

 0031-9007/98/80(9)/1900(4)$15.00

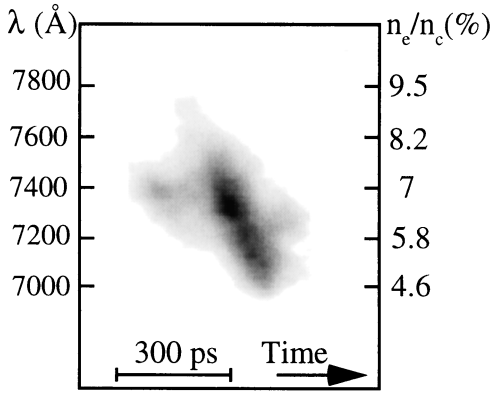

FIG. 1. Time-resolved spectrum of stimulated Raman backscattering of the interaction laser beam. Electron densities are deduced from the resonance relations of the Raman decay and the linear equations of dispersion of the waves, using an electron temperature of 0.7 keV.

was focused with an $f/3$ lens and a RPP with 1.5 mm square elements. The focal spot diameter was 110 μm (FWHM), with a maximum average intensity of $I_{\text{pump}} = 3 \times 10^{14}$ W/cm^2. The speckles generated by the RPP on the interaction beam had a mean diameter of 3 μm (minimum to minimum) and a mean length of 32 μm. During the interaction pulse, the plasma density was below critical electron density (critical density for $\lambda_0 = 0.53$ μm light is $n_c = 4 \times 10^{21}$ cm^{-3}). The electron density profile had an approximately parabolic shape along the laser axis with a scale length of $\sim$300 μm, with the maximum density on axis decreasing from $0.1n_c$ to $0.06n_c$ during the first 300 ps of the interaction pulse. Characterization of electron density and temperature of the plasma was done using time-resolved spectra of stimulated Raman scattering in the backward direction. An example of a Raman spectrum is shown in Fig. 1. Electron density on the laser axis was deduced from the temporal evolution of the long wavelength edge of the spectra, and an electron temperature (T_e) of 0.7 keV was deduced from the Landau cutoff of the Raman spectra.

The diagnostic to measure the space resolved SBS consisted of a three-frame gated optical imager (GOI). This instrument yields three two-dimensional images with a temporal resolution of 150 ps, with an adjustable delay between frames, which was chosen to be 200 ps. During the first phase of the experiment, the focal spot produced by the RPP was characterized in the absence of plasma by imaging the beam waist of the transmitted laser light. This was recorded using the same GOI instrument. During the second phase, the GOI detector assembly was installed in the back scattering diagnostic station, to measure the space distribution of the SBS emission. The spatial resolution was 5–10 μm. The experimental arrangement is illustrated in Fig. 2, showing simultaneously the optical configurations to characterize the focal spot, and to image the far-field distribution of SBS in the backscattered direction. The RPP on the interaction beam was placed before the beam splitter that collected the backscattered light, to permit undisturbed imaging of SBS emission. Time-resolved SBS spectra and absolute SBS reflectivities were also measured in the backscattering direction of the interaction beam.

The laser intensity distribution at the beam waist of the focal spot in the absence of plasma is shown in Fig. 3. Since the actual location and intensities of the individual speckles vary from time to time due to fluctuations in the optical characteristics of the laser beam, a direct comparison on the location of the speckles and SBS emission is not possible (since only one GOI instrument was available), but the statistical distribution of speckles as a function of intensity will be the same during the experiment. Figure 4 shows the far-field SBS intensity distribution at three different times during the interaction pulse ($t = 1.2$ ns corresponds to the peak of the interaction beam). The data show the localized nature of the SBS reflectivity, with major contributions to the overall reflectivity coming from a few well-defined regions, located mainly in the central part of the focal spot. Some correlation in time of the location of SBS emission can be observed in the three frames. It

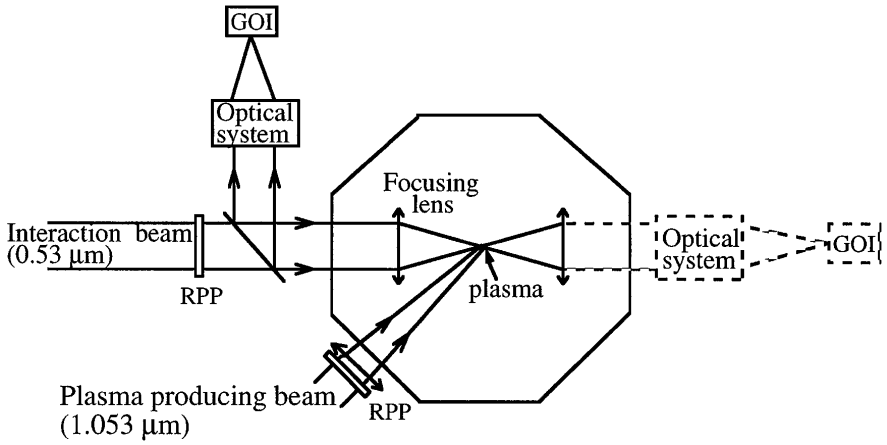

FIG. 2. Experimental arrangement for the GOI diagnostic to measure either the laser intensity distribution at best focus or the space distribution of the SBS emission.

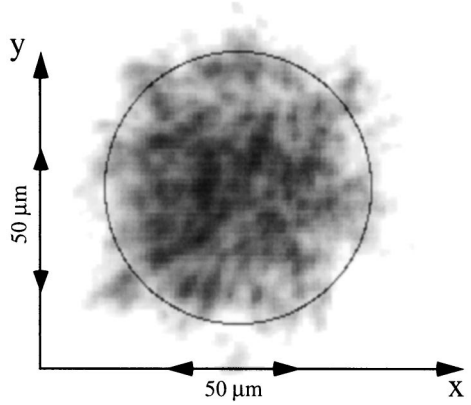

FIG. 3. Spatial laser intensity distribution at the beam waist of the focal spot in the absence of plasma. The circle has a diameter of 100 μm.

was observed that the SBS growth was localized in small regions and persisted for times longer than 200 ps, but shorter than the laser pulse duration.

From these images, the SBS emission was analyzed in detail to obtain the local peak reflectivities and to compare them to the total, or average in time and space, SBS reflectivity. This latter was low, typically between 10^{-4} and 10^{-5}, due to plasma conditions, low laser intensities, and the use of a 0.53 μm laser pump. The SBS emission from the individual spots shown in Fig. 4 was evaluated, given the local brightness of the emitting spots. For the data shown in frame 2 of Fig. 4, only $1/100$ of the area of the focal spot contributed to the measured reflectivity. The SBS hot spot, marked *A* in Fig. 4, contains approximately 50% of the total reflected light, implying that the peak localized SBS emission was higher than the average reflectivity by a factor between 50 and 100. If one takes into account the temporal evolution of the SBS emission, one ends with even higher peak reflectivities. The localized SBS emission, as indicated in Fig. 4, does not necessarily imply that these are due to single speckle contributions. Because of optical integration along the laser axis and over the optical resolution of the system, the SBS emission from one spot could be the result of the superposition of contributions from more than one speckle.

The spectrum of the backscattered SBS light was analyzed as a function of time. The time-resolved SBS spectrum, from the same shot as the GOI images of Fig. 4, is shown in Fig. 5. It is redshifted from the laser wavelength, with a shift and a broadening increasing as a function of time. Using the velocity profile from two-dimensional hydrodynamics simulations, we observe that SBS starts around the isothermal sonic point, which is located $\sim$100 μm in front of the summit of the density profile, and then the region of SBS emission extends towards the peak of the profile up to $\sim$100 μm on the back of the target.

The SBS reflectivities, local and average, were calculated using a statistical approach [4,6,8] which had been applied to the experiment using electron density, electron temperature, and velocity profiles provided by two-dimensional hydrodynamic simulations. The basic assumption of the statistical SBS theory [4] is that the scattered radiation is generated in several independent speckles, rather than homogeneously over the illuminated region of plasma. The first step of this theory is to calculate the integrated reflectivity from a single speckle, using the known SBS linear theory in stationary convective regime [7], taking into account diffraction of scattered light in the speckle and pump depletion [8]. The reflectivity of the single speckle is then averaged over the statistical distribution of speckles with different intensities in the interaction region [6,8].

The SBS intensity has been calculated according to this model, and shows reasonable agreement with the experiment for the total SBS reflectivity (5×10^{-4}) as well as for its temporal evolution and location. The model used the profiles given by the numerical simulation, which provided good agreement with the experiment for the temporal evolution of the electron density on the laser axis as measured from the Raman spectra. More recent experiments [9] have shown improved agreement between experiment and modeling for SBS reflectivities when using

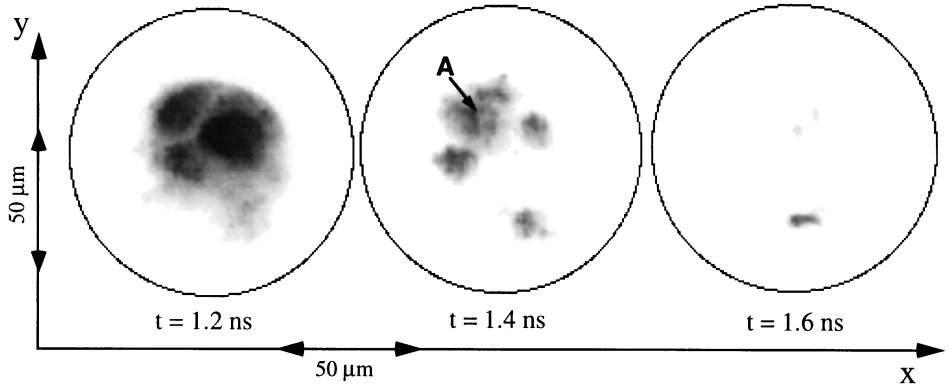

FIG. 4. Spatial intensity distribution of the SBS emission at three different times during the interaction pulse. These images are integrated over 150 ps; $t = 1.2$ ns corresponds to the peak of the interaction beam. The circles are positioned in the same way as in Fig. 3, and have a diameter of 100 μm.

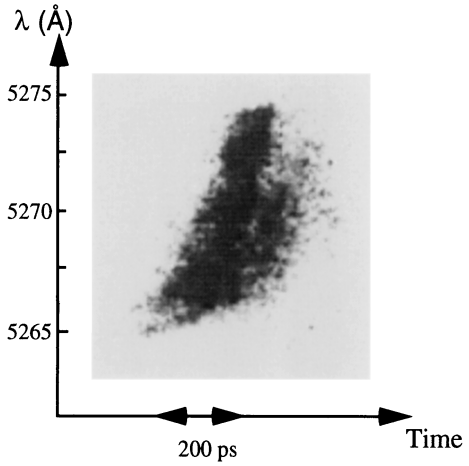

FIG. 5. Time-resolved spectrum of the SBS light collected in the focusing optics of the interaction beam. In the SBS decay, the frequency of the SBS light is given by $\omega_{\mathrm{SBS}} = \omega_0 - \omega_{\mathrm{iaw}}$, and the wavelength shift of the SBS light compared to the laser light is $\delta\lambda = (\lambda_0^2/2\pi c)k_{\mathrm{iaw}}(c_s - u)$, where k_{iaw} is the wave number of the ion acoustic wave, c_s is the sound speed, and u is the expansion velocity. The pump laser wavelength is $\lambda_0 = 5265$ Å.

the experimental shape of the electron density profile, and temperature, measured with a Thomson scattering diagnostic. At the time of SBS maximum activity, the maximum emission comes from a region $z = -20$ μm from the plasma center and has an extent of about 120 μm FWHM. This area corresponds to the subsonic plasma expansion, in agreement with the observed redshift of the SBS spectrum.

The average SBS gain is very low for the parameters of this experiment: $\langle G\rangle = 4.6 \times 10^{-16}[\langle I\ (\mathrm{W/cm^2})\rangle \times \lambda_0\ (\mu\mathrm{m})\ L_v\ (\mu\mathrm{m})\ n_e/n_c]/(1 - n_e/n_c)[T_e\ (\mathrm{keV}) + 3 \times T_i\ (\mathrm{keV})/Z] \leq 1$ (L_v is the velocity gradient scale length, T_i is the ion temperature), for which the expected SBS reflectivity should be extremely small if it would not be for the presence of the statistical distribution of intensities associated with the speckled structure of the focal spot. Taking into account this gain, we can study the contribution of speckles with different intensities to the SBS reflectivity. This is a growing function of the speckle relative intensity ($u = I/\langle I\rangle$), which ends abruptly at $u = 11$ because the expected number of speckles in the interaction volume with higher intensities than this value is less than 1. Most of the SBS emission comes from speckles with intensities u between 10 and 11. If the spatial resolution of the instrument would be able to resolve one speckle, the maximum local reflectivity that would be measured will be as high as 0.15–0.2, which is about 2000 times larger than the average SBS reflectivity. For the case of the experiment, the optical resolution Δ_0 was larger than a speckle diameter d_0 so the maximum observed reflectivity decreases as the square of the ratio of the spatial resolution to the speckle diameter: $R_{\mathrm{measured}} = R_{\mathrm{max}}(d_0/\Delta_0)^2$. Hence, for an instrumental resolution of about 10 μm, the maximum intensity will be ~200 times above the average, which is close to the experimental result.

In summary, we have presented the first detailed experimental characterization of the far-field distribution of the SBS reflectivity, showing that the emission comes from very small regions defined by the laser intensity distribution due to the RPP used in the focusing optics. Modeling of both the average and local reflectivities gives values that are very close to the experimental values, demonstrating the importance of considering the microscopic nature of the interaction. This experiment demonstrates clearly the need for detailed evaluation of the reflectivity of SBS as a function of space and time, if one is to attempt to compare experimental results with existing theoretical models. This also applies to other instabilities such as stimulated Raman scattering.

The authors gratefully acknowledge valuable discussions with Joseph Kilkenny, Kent Estabrook, and Sham Dixit, and the support of the technical groups of LULI. This work was partially supported under the auspices of the U.S. Department of Energy by the Lawrence Livermore National Laboratory under Contract No. W-7405-ENG-48. Part of this support was provided through the LLNL-LDRD program under the Institute for Laser Science and Applications.

*Present address: CEA Limeil-Valenton, 94195 Villeneuve St. Georges Cedex, France.
†Permanent address: P. N. Lebedev Physics Institute, Russian Academy of Science, Moscow 117924, Russia.

[1] W. L. Kruer, *The Physics of Laser Plasma Interactions* (Addison-Wesley, Redwood City, CA, 1988).
[2] H. A. Baldis, E. M. Campbell, and W. L. Kruer, in *Laser-Plasma Interactions*, Handbook of Plasma Physics (North-Holland, Amsterdam, 1991), pp. 361–434.
[3] W. L. Lindl, Phys. Plasmas **2**, 3933 (1995).
[4] H. A. Rose and D. F. DuBois, Phys. Fluids B **5**, 590 (1993); H. A. Rose and D. F. DuBois, Phys. Rev. Lett. **72**, 2883 (1994); H. A. Rose, Phys. Plasmas **2**, 2216 (1995).
[5] Y. Kato, K. Mima, N. Miyanaga, S. Arinaga, Y. Kitagawa, M. Nakatsuka, and C. Yamanaka, Phys. Rev. Lett. **53**, 1057 (1984).
[6] V. T. Tikhonchuk, C. Labaune, and H. Baldis, Phys. Plasmas **3**, 3777 (1996).
[7] L. M. Gorbunov and A. N. Polyanichev, Sov. Phys. JETP **47**, 290 (1978); A. Ramani and C. E. Max, Phys. Fluids **26**, 1079 (1983).
[8] V. T. Tikhonchuk, D. Pesme, and Ph. Mounaix, Phys. Plasmas **4**, 2658 (1997).
[9] C. Labaune, H. Baldis, and V. T. Tikhonchuk, Europhys. Lett. **38**, 31 (1997).